JOURNAL OF SOLID STATE CHEMISTRY **59**, 133–142 (1985)

Luminescence of Bi^{3+}-Doped Crystals of Cs_2NaYBr_6 and $Cs_2NaLaCl_6$

A. WOLFERT AND G. BLASSE

*Physical Laboratory, State University Utrecht, P.O. Box 80.000,
3508 TA Utrecht, The Netherlands*

Received September 10, 1984

The luminescence properties of Cs_2NaYBr_6–Bi^{3+} and $Cs_2NaLaCl_6$–Bi^{3+} crystals are reported. Emission is observed from isolated Bi^{3+} ions and from Bi^{3+} pairs. For the isolated Bi^{3+} ion the emissions are in the ultraviolet region. Excitation in the *A* band yields only $^3T_{1u}$ emission in case of Cs_2NaYBr_6–Bi^{3+} and $^3T_{1u}$ and $^3A_{1u}$ emission in case of $Cs_2NaLaCl_6$–Bi^{3+}. Decay time measurements as a function of temperature are also reported. © 1985 Academic Press, Inc.

1. Introduction

The luminescence properties of the Bi^{3+} ion ($6s^2$ configuration) have been studied in many host lattices (*1–5*). It appeared that the nature of the Bi^{3+} luminescence depends strongly on the host lattice. The emission of the Bi^{3+} ion can be in the ultraviolet region, but also in the red region, dependent on the host lattice.

The luminescence of monovalent s^2 ions (like Ga^+, In^+, Tl^+) in alkali halides has been studied extensively. Theoretical treatments are mainly available for these systems (*6, 7*). In the alkali halides the monovalent s^2 ions are octahedrally coordinated by the halogen ions. The ground state of the ion is $^1S_0$. The excited state gives rise to four states: $^3P_0$, $^3P_1$, $^3P_2$ and $^1P_1$. For an ion in a cubic crystal field the Mulliken notation is used, viz., $^1A_{1g}$, $^3A_{1u}$, $^3T_{1u}$, $^3E_u + {}^3T_{2u}$, and $^1T_{1u}$. The transition $^1A_{1g} \rightarrow {}^1T_{1u}$ is allowed (*C* band). The transition $^1A_{1g} \rightarrow {}^3A_{1u}$ is forbidden, the transition $^1A_{1g} \rightarrow {}^3T_{1u}$ is partially allowed (*A* band) by spin–orbit interaction. The transition $^1A_{1g} \rightarrow {}^3E_u + {}^3T_{1u}$ (*B* band) is forbidden, but can be induced by lattice vibrations. Upon excitation into the *A* band in general two emission bands are observed, viz., the so-called A_X and A_T emission. The origin of these two emissions is the existence of two minima on the adiabatic potential energy surface of the $^3T_{1u}$ relaxed excited state. These minima are due to the Jahn Teller coupling of the orbital triplet to the ε_g and τ_{2g} lattice modes (*6, 7*).

It can be imagined that in case of the luminescence of the Bi^{3+} ion the same model is valid. Because the theoretical models are based upon s^2 ions octahedrally coordinated by halogen ions, it is necessary to study the luminescence of the Bi^{3+} ion in these coordinations. It is not possible to study the Bi^{3+} luminescence in alkali halides, because in the alkali halides the Bi^{3+} ion replaces a monovalent ion and charge compensation is required. This charge compensation will certainly lower the site symmetry of the Bi^{3+} ion. For this reason the cubic elpasolites Cs_2NaLnX_6 (with *Ln* = La–Lu and *X* = Cl or Br) are proper host lattices. In these lattices the LnX_6^{3-} octahedra do not share halogen ions with each other. The octahedra are known

0022-4596/85 $3.00

to be perfectly cubic (*8, 9*). The compound $Cs_2NaBiCl_6$ has also this structure (*10*). For this reason the luminescence of Cs_2NaYCl_6–Bi^{3+} (*11*) was studied. It appeared that the Stokes shift of the emission was very small and the excitation spectra as well as the emission spectra showed extended vibrational structure. This vibrational structure could be assigned to vibrations of the isolated $BiCl_6^{3-}$ octahedra and lattice vibrations.

In continuation of that work the luminescence properties of Cs_2NaYBr_6–Bi^{3+} and $Cs_2NaLaCl_6$–Bi^{3+} are described in this paper. The compound Cs_2NaYBr_6 has the same crystal structure as Cs_2NaYCl_6 (*12*). The compound $Cs_2NaLaCl_6$ at room temperature also has this structure, but it shows a phase transition at a temperature below room temperature (*13*). The $LaCl_6^{3-}$ octahedra rotates about the [001] axis over a small angle (between 5 and 10°). The octahedral coordination of the La^{3+} ion by the chloride ions remains the same.

The results reported in this paper are compared to the earlier work on Cs_2NaYCl_6–Bi^{3+}. It is also possible to make a comparison between these three Bi^{3+}-doped systems and the Tl^+ ($6s^2$)-doped alkali halides.

2. Experimental

2.1. Crystal Growth

The crystals of Cs_2NaYBr_6–Bi^{3+} and $Cs_2NaLaCl_6$–Bi^{3+} were prepared in the same way as the crystals of Cs_2NaYCl_6–Bi^{3+} (*10, 11, 14*). Starting materials were CsCl (Merck, optipur), CsBr (Merck, optipur), NaCl (Merck, p.a.), NaBr (Merck, p.a.), Y_2O_3 (Highways International 99.999%) and La_2O_3 (Highways International 99.999%). The Bi^{3+} dope was added as $Cs_3Bi_2X_9$ (with X = Cl or Br) (*15, 16*) compensated with CsX (X = Cl or Br) and NaX (X = Cl or Br). Stoichiometric quantities of the compound and the dopant were dissolved in concentrated HCl (Baker, analyzed) or HBr (Baker, analyzed). After evaporation the salt was dried under vacuum at 200°C for 48 hr. The salt is molten under an HX (X = Cl or Br) atmosphere and filtered through a quartz filter (G3) into a quartz ampulla. Crystals were grown by the Stockbarger method. Samples were prepared by cutting the crystals in pieces of $0.5 \times 0.5 \times 0.5$ cm^3. The surfaces were polished with diamond lapping powder (3 μm). These handlings were carried out in a dry nitrogen atmosphere, because the materials are highly hygroscopic. The crystals were checked by X-ray diffraction using Cu$K\alpha$ radiation. According to the IR spectra of the 3-μm region the crystals did not contain water or OH^-. The Bi^{3+} concentration in the crystals was determined by atomic absorption spectrometry.

2.2. Instrumentation

The emission and excitation spectra were recorded using a Perkin–Elmer MPF-44L spectrofluorometer (spectral resolution ~0.4 nm). This apparatus was equipped with an Oxford Instruments CF204 liquid helium flow cryostat. The excitation spectra were corrected for the lamp intensity and the transmittance of the monochromator with the use of Lumogen T-rot GG as a standard (*17*). The emission spectra were corrected for the photomultiplier sensitivity. The photon flux per constant energy interval (Φ) is obtained by multiplying the radiant power per constant wavelength interval by λ^3.

The decay time measurements were performed with the use of an EG&G photon counting system. The excitation source is a pulsed Xe lamp (EG&G 108 AU) with a pulse width of ~1 μsec. Excitation wavelengths are selected by bandpass filters and cutoff filters. Emission wavelengths are selected by a double monochromator (Jobin Yvon, HRD1). The signal is detected by a photomultiplier tube (RCA C31034). The

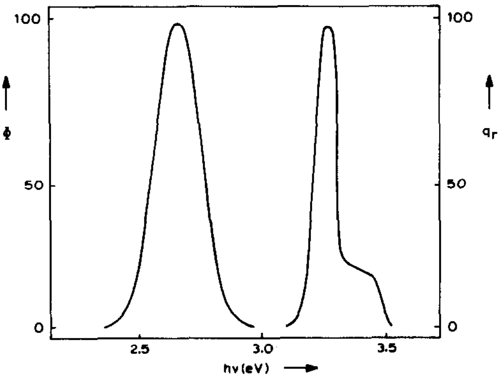

FIG. 1. Emission and excitation spectra of Cs_2NaYBr_6–Bi^{3+} [0.03 at.%] at 4.2 K. The emission spectrum is recorded upon excitation at 3.27 eV. The excitation spectra are recorded for emission at 2.66 eV; Φ denotes the photon flux per constant energy interval in arbitrary units; q_r denotes the relative quantum output in arbitrary units.

signal is analysed by a multichannel analyzer (EG&G Ortec 7100) in the multichannel scaling mode (time per channel 1 μsec). The multichannel analyzer is triggered with pulses generated directly from the lamp flash by a photodiode.

3. Results

3.1. Cs_2NaYBr_6–Bi^{3+}

For the crystals of Cs_2NaYBr_6–Bi^{3+} two luminescent centers are observed at 4.2 K. One center has its emission band at 2.66 eV (Fig. 1). The excitation spectrum of this emission consists of two bands: one at 3.27 eV and a weaker band at 3.40 eV. The intensity of the latter depends on the Bi^{3+} concentration in the crystals. For crystals with higher Bi^{3+} concentrations the intensity of the 3.40 eV excitation band increases relative to that of the 3.27 eV band.

For the other center two emission bands are observed at 4.2 K, viz., a single emission band at 3.16 eV and a band with a weak vibronic structure with its maximum at 3.08 eV (Fig. 2). The excitation spectrum shows three bands at 3.36, 4.25, and 4.82 eV (Fig. 3). Excitation at 3.36 eV yields only the single emission band at 3.16 eV. Excitation at 4.25 and 4.82 eV results in the emissions at 3.16 and 3.08 eV.

The intensity of the 3.16 eV (and 3.08 eV) emission relative to the intensity of the 2.66-eV emission depends on the Bi^{3+} concentration in the crystal. For crystals with higher Bi^{3+} concentration the intensity of the 2.66 eV emission increases relative to that of the 3.16 eV emission. The intensity of both emissions as a function of temperature is given in Fig. 4 for a crystal containing about 300 ppm Bi^{3+}. Quenching of the 3.16-eV emission starts at about 40 K. The same is observed for lower Bi^{3+} concentrations.

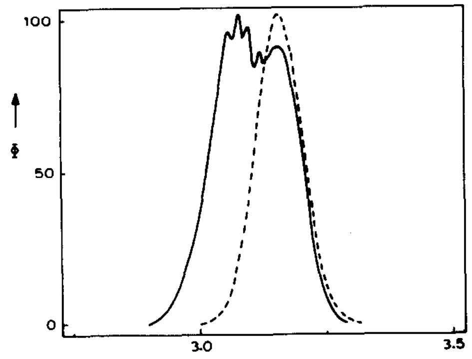

FIG. 2. Emission spectra of Cs_2NaYBr_6–Bi^{3+} [0.06 at.%] at 4.2 K. (—) excitation at 4.25 eV [*D* band]; (---) excitation at 3.36 eV [*A* band].

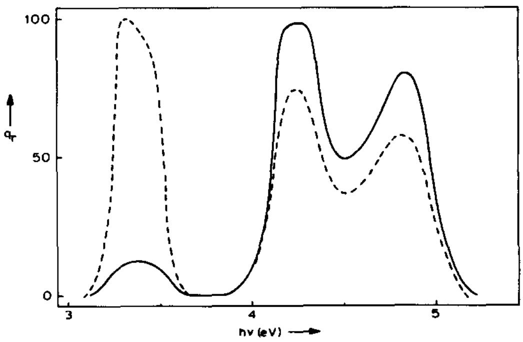

FIG. 3. Excitation spectra of Cs_2NaYBr_6–Bi^{3+} [0.06 at.%] at 4.2 K. (—) emission at 3.08 eV [$^3A_{1u}$]; (---) emission at 3.16 eV [$^3T_{1u}$].

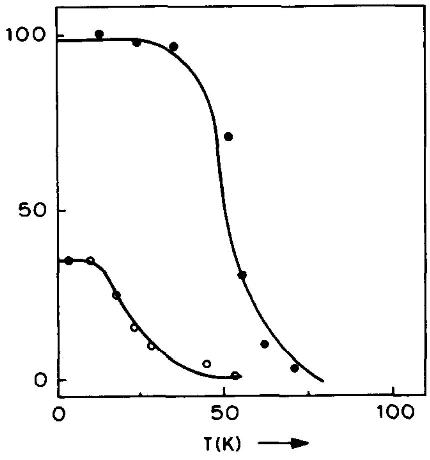

FIG. 4. Luminescence intensity as a function of temperature for Cs_2NaYBr_6–Bi^{3+} [0.06 at.%]. (●) excitation at 3.36 eV, emission at 3.08 eV; (○) excitation at 3.27 eV, emission at 2.66 eV.

Decay time measurements were performed upon excitation at 3.36 and 4.25 eV. All decay curves are exponential. The decay time of the 3.16-eV emission (excitation at 3.36 eV) is short (≤ 1 μsec) at 4.2 K. The decay time of the emission at 3.08 eV (excitation at 4.25 eV) is 580 μsec at 4.2 K. This decay time is given in Fig. 5 as a function of temperature.

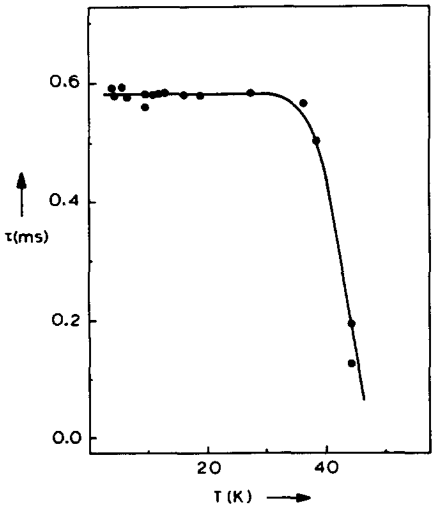

FIG. 5. Decay time of the 3.08-eV emission of Cs_2NaYBr_6–Bi^{3+} [0.06 at.%] as a function of temperature. Excitation energy at 4.25 eV.

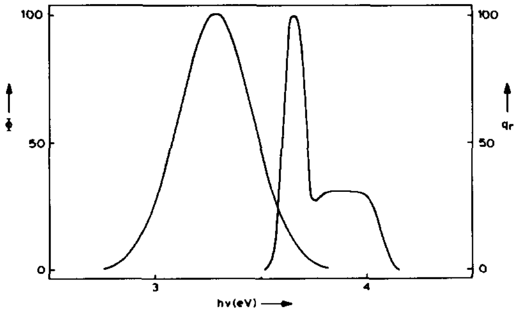

FIG. 6. Excitation and emission spectra of $Cs_2NaLaCl_6$–Bi^{3+} [0.03 at.%] at 4.2 K. The emission spectrum is recorded upon excitation at 3.76 eV. The excitation spectrum is recorded for emission at 3.28 eV.

3.2. $Cs_2NaLaCl_6$–Bi^{3+}

As for Cs_2NaYBr_6–Bi^{3+}, two luminescent centers are observed for $Cs_2NaLaCl_6$–Bi^{3+} at 4.2 K. These two centers resemble the centers observed for Cs_2NaYBr_6–Bi^{3+}. One center has its emission band at 3.28 eV (Fig. 6). The excitation spectrum of this center shows a band at 3.76 eV and an excitation region between 3.80 and 4.10 eV. The intensity of this latter region relative to the 3.76-eV band increases for crystals with higher Bi^{3+} concentrations.

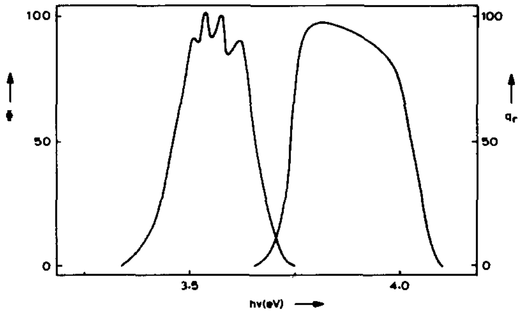

FIG. 7. Excitation and emission spectra of $Cs_2NaLaCl_6$–Bi^{3+} [0.03 at.%] at 4.2 K. The emission spectrum is recorded upon excitation at 3.90 eV. The excitation spectrum is recorded for emission at 3.60 eV.

The other center shows two emission bands (Fig. 7): one at 3.63 eV and another band, with a weak vibronic structure, with a maximum at about 3.53 eV. The excitation is in the region 3.70–4.10 eV. The

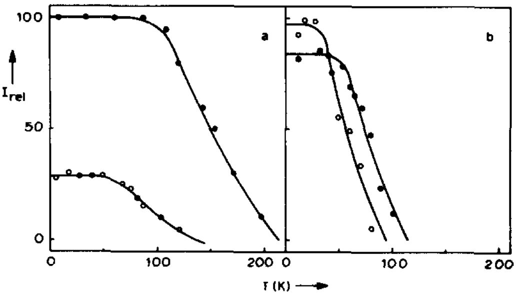

FIG. 8. Luminescence intensity as a function of temperature for $Cs_2NaLaCl_6$–Bi^{3+} [0.03 at.%] (a) and for $Cs_2NaLaCl_6$–Bi^{3+} [0.4 at.%] (b). (●) excitation at 3.90 eV, emission at 3.60 eV; (○) excitation at 3.76 eV, emission at 3.28 eV.

intensity of the 3.28-eV emission relative to the 3.53-eV emission depends on the Bi^{3+} concentration in the crystal, just like in the case of Cs_2NaYBr_6–Bi^{3+}. The intensity of both emissions as a function of temperature is given in Fig. 8. From this figure it is obvious that the temperature at which quenching of the emission occurs depends on the Bi^{3+} concentration. All decay curves appeared to be exponential. The decay time of the emission upon excitation at 4.0 eV is about 2.4 msec at 4.2 K. The decay time as a function of temperature is given in Fig. 9.

4. Discussion

From the results it should be clear that one of the two centers observed in Cs_2NaYBr_6–Bi^{3+} as well as in $Cs_2NaLaCl_6$–Bi^{3+} can be ascribed to isolated Bi^{3+} ions, while the other can be ascribed to Bi^{3+} pairs or simple Bi^{3+} clusters.

The centers with the lower energy emission and the larger Stokes shifts are assumed to be the Bi^{3+} pairs. Luminescence from Bi^{3+} pairs has been observed before, for example in YOCl–Bi^{3+} (*18*) and $LaBO_3$–Bi^{3+} (*19*). The Stokes shift for the pair emission in these two compounds is about 1.9 eV. Since the relevant distance is about 3.4 Å for YOCl–Bi^{3+} and for $LaBO_3$–Bi^{3+}, this suggests that the Stokes shift is determined mainly by the Bi^{3+}–Bi^{3+} distance. However, for LaB_3O_6–Bi^{3+} (*20*) the Bi^{3+}–Bi^{3+} distance is about 4 Å, but the Stokes shift amounts to 0.6 eV. The Stokes shifts of the pair emissions in Cs_2NaYBr_6–Bi^{3+} and $Cs_2NaLaCl_6$–Bi^{3+} are 0.61 and 0.48 eV, respectively. The shortest Bi^{3+}–Bi^{3+} distance in these lattices is about equal, viz., 7.8 Å, while the Stokes shifts differ. Apparently not only the Bi^{3+}–Bi^{3+} distance determines the luminescence properties of the Bi^{3+} pairs, but also the nature of the coordinating anions. The shoulder on the high energy side of the excitation band of the pairs agrees well with the excitation band of the isolated Bi^{3+} ions, for both systems. This suggests energy transfer from single ions to pairs. This is very possible because of the large spectral overlap of the emission band of the isolated Bi^{3+} ions and the excitation band of the Bi^{3+} pairs.

In the following section we concentrate on the luminescence of the isolated Bi^{3+} ions.

4.1. Cs_2NaYBr_6–Bi^{3+}

The excitation band at 3.36 eV is ascribed

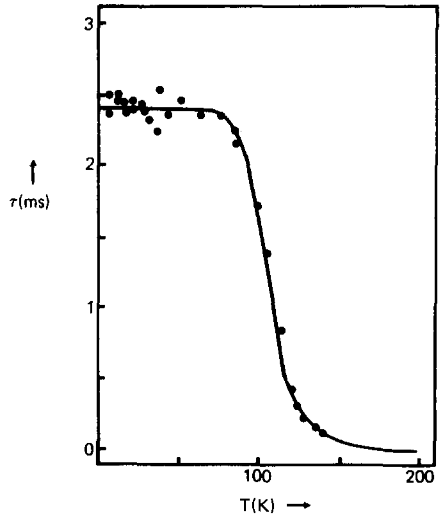

FIG. 9. Decay time of the 3.08-eV emission of $Cs_2NaLaCl_6$–Bi^{3+} [0.008 at.%] as a function of temperature. Excitation energy at 4.0 eV.

to the ${}^1A_{1g} \rightarrow {}^3T_{1u}$ transition (the so-called A band). Compared to Cs_2NaYCl_6–Bi^{3+}, where this excitation band is at 3.85 eV (*11*), it is shifted about 0.45 eV to lower energy. According to Jørgensen (*21*) the ${}^1S_0$–${}^3P_1$ absorption band shifts 0.46 eV going from chlorides to bromides. These values agree satisfactorily.

The excitation band at 4.82 eV can be ascribed to the ${}^1A_{1g} \rightarrow {}^1T_{1u}$ transition (the so-called C band). In that case the energy difference between the ${}^1T_{1u}$ state and the ${}^3T_{1u}$ state amounts to about 1.50 eV, which is in good agreement with the data from Jørgensen (*21*). For the excitation band at 4.25 eV two assignments are possible. The first one is that the excitation band belongs to the ${}^1A_{1g} \rightarrow {}^3E_u + {}^3T_{2u}$ transition (the so-called B band). This assignment is not probable, because the B band is not observed in Cs_2NaYCl_6–Bi^{3+} nor in $Cs_2NaLaCl_6$–Bi^{3+}. A more likely assignment is that the 4.25 eV excitation band belongs to the charge-transfer transition (so-called D band). It is known that in bromides the charge transfer from the Br^- ion to the Bi^{3+} ion is at relatively low energy. Examples of this are $K_4Bi_2Br_6 \cdot 2H_2O$ (*22*), Rb_3BiBr_6 (*22*), and LaOBr–Bi^{3+} (*23*).

The emission upon excitation at 3.36 eV is ascribed to the ${}^3T_{1u} \rightarrow {}^1A_{1g}$ transition. The decay time of this emission is short, which should be expected for an allowed transition. Upon excitation at 4.25 eV two emission bands are observed. One is at 3.16 eV and is identical to the emission after excitation at 3.36 eV. The other emission band at 3.08 eV is ascribed to the ${}^3A_{1u} \rightarrow {}^1A_{1g}$ transition. Because this transition is forbidden, the decay time of the emission has to be long. The decay time at 4.2 K (upon excitation at 4.25 eV) is about 580 μsec, which confirms the assignment.

On the ${}^3A_{1u} \rightarrow {}^1A_{1g}$ emission band some vibronic lines are observed. The energy differences between these lines are equal within the accuracy of the experiment; their value is (160 ± 10) cm^{-1}. We note that also in the case of Cs_2NaYCl_6–Bi^{3+} the vibronic structure is more pronounced in the ${}^3A_{1u} \rightarrow {}^1A_{1g}$ emission than in the ${}^3T_{1u} \rightarrow {}^1A_{1g}$ emission. The different electron-lattice coupling in the ${}^3A_{1u}$ state and the ${}^3T_{1u}$ state is, in this strong spin-orbit coupling case, probably due to the mixing of the ${}^1T_{1u}$ state and the ${}^3T_{1u}$ state, which is not possible for the ${}^3A_{1u}$ state. The vibronic structure is ascribed to vibrations of the $BiBr_6^{3-}$ octahedron. For Cs_2NaYCl_6–Bi^{3+} extended vibrational structure in the emission and excitation spectra was observed (*11*). The vibronic structure could be assigned to internal modes of the $BiCl_6^{3-}$ octahedron and to lattice modes. The highest frequencies obtained from the spectra amounted to 295 (ν_1), 200 (ν_2), and 110 (ν_3) cm^{-1}. If we correct the values for ν_1 and ν_2 for the replacement of chlorine by bromine, we arrive at 197 and 133 cm^{-1}, respectively. Since the force constants in the bromide will also be lower than in the chloride, we ascribe the experimental value of 160 cm^{-1} to the ν_1 mode. The vibrational structure in the emission spectrum of Cs_2NaYBr_6–Bi^{3+} is much weaker than for Cs_2NaYCl_6–Bi^{3+}. The Stokes shift of the emission of Cs_2NaYBr_6–Bi^{3+} is larger than for Cs_2NaYCl_6–Bi^{3+}, due to the larger space available for the Bi^{3+} ion (*19*). In terms of a configurational coordinate diagram, the offset of the parabolae Δr is larger for the bromide than for the chloride. This larger offset results also in a weaker vibronic structure.

The energy difference between the ${}^3A_{1u}$ level and the ${}^3T_{1u}$ level can be obtained from the emission spectrum. It amounts to about (650 ± 50) cm^{-1}. The largest phonon available from the $BiBr_6^{3-}$ octahedron is about 160 cm^{-1}. At least four phonons are required to overcome the energy difference between the ${}^3T_{1u}$ level and the ${}^3A_{1u}$ level. Obviously, this makes the probability for this nonradiative transition so small that excitation into the ${}^3T_{1u}$ level results only in ${}^3T_{1u}$ emission.

No $^3A_{1u}$ emission is observed. These observations are in line with those on Cs_2NaYCl_6–Bi^{3+} in which lattice also four phonons were required to overcome the energy difference between the $^3T_{1u}$ level and the $^3A_{1u}$ level.

Upon *C* and *D* band excitation emission from $^3A_{1u}$ is observed. It has to be assumed that the $^3A_{1u}$ level is populated directly by the higher levels and not by the $^3T_{1u}$ level.

The decrease of τ at higher temperatures must be due to thermal quenching of the luminescence (compare Figs. 4 and 5).

Quenching of the 3.16 eV emission is probably due to nonradiative processes in the center itself. For crystals containing 0.060 and 0.015 at.% Bi^{3+} the same quenching temperature is observed. This makes it unlikely that quenching of the luminescence is due to energy migration. The quenching temperature of the luminescence in Cs_2NaYBr_6–Bi^{3+} is much lower than for the corresponding chloride compound ($T_q > 100$ K) *(11)*. We feel that the low-lying charge transfer state in the bromide compound may be responsible for the low quenching temperature. A low quenching temperature of the Bi^{3+} luminescence is also observed in other bromide compounds, e.g., $K_4Bi_2Br_{10}$ *(22)*, Rb_3BiBr_6 *(22)*, and $CsCdBr_3$–Bi^{3+} *(24)*.

The low-temperature decay time of the $^3A_{1u}$ emission is relatively short (~580 μsec) compared to the decay time of the $^3A_{1u}$ emission in $Cs_2NaLaCl_6$–Bi^{3+}. Two explanations are possible. The first one is that due to the low-lying charge-transfer state nonradiative processes are already important at 4.2 K. The other possibility is that the charge-transfer state mixes with the states of the Bi^{3+} ion, making the transition $^3A_{1u} \rightarrow {}^1A_{1g}$ less forbidden. At this moment it is not possible to decide which explanation is correct.

Comparing the luminescence properties of Cs_2NaYBr_6–Bi^{3+} and those of Cs_2NaYCl_6–Bi^{3+} a few conclusions can be made. The Stokes shift for the bromide compound is larger than for the chloride compound due to the larger space available in the bromide lattice for the Bi^{3+} ion. The larger relaxation in the case of the bromide, which is responsible for the larger Stokes shift, results also in a weaker vibronic structure in the emission and excitation spectrum. The energy difference between the $^3T_{1u}$ and the $^3A_{1u}$ levels is smaller in case of Cs_2NaYBr_6–Bi^{3+}. Because the phonons available in the bromide lattice are also smaller than in the chloride lattice, the nonradiative transition $^3T_{1u} \rightarrow {}^3A_{1u}$, after excitation in the *A* band, cannot compete with the radiative transition $^3T_{1u} \rightarrow {}^1A_{1g}$.

4.2. $Cs_2NaLaCl_6$–Bi^{3+}

For the isolated Bi^{3+} ions in $Cs_2NaLaCl_6$–Bi^{3+} only one excitation band and two emission bands are observed. The excitation band region at 3.70–4.10 eV is ascribed to the $^1A_{1g} \rightarrow {}^3T_{1u}$ transition. The position of this band is comparable to the position of this band for Cs_2NaYCl_6–Bi^{3+} (3.80 eV). The shape of the excitation band is remarkable. A real maximum is not observed. This is probably due to the relatively high Bi^{3+} concentration in our crystals (viz., 0.4 and 0.03 at.%). The excitation band belonging to the $^1A_{1g} \rightarrow {}^1T_{1u}$ transition should be expected at 5.60 eV, which is not in the spectral reach of the apparatus used. The energy difference between the $^3T_{1u}$ level and the $^1T_{1u}$ level is about 1.74 eV in case of Cs_2NaYCl_6–Bi^{3+}. According to Jørgensen *(21)* this difference amounts to 1.80 eV in case of Bi^{3+}-chloride complexes.

Upon excitation at 4.00 eV two emission bands are observed. One band has its maximum at 3.63 eV and the other band has its maximum at about 3.53 eV. This latter band shows a weak vibrational structure. The energy differences between the vibronic lines amount to 290 ± 10 and 260 ± 10 cm^{-1}. These values are in line with the observations for the emission spectrum of Cs_2NaY

Cl_6–Bi^{3+} (see above). In view of the small number of lines available, further analysis is impossible. The 3.63-eV emission is ascribed to the $^3T_{1u} \rightarrow {}^1A_{1g}$ transition and the 3.53-eV emission to the $^3A_{1u} \rightarrow {}^1A_{1g}$ transition. The energy difference between the $^3T_{1u}$ level and the $^3A_{1u}$ level amounts to about (800 ± 80) cm^{-1}.

The largest phonon frequency available is about 300 cm^{-1}. For the nonradiative transition $^3T_{1u} \rightarrow {}^3A_{1u}$ about three phonons are required making the nonradiative rate higher than in case of Cs_2NaYBr_6–Bi^{3+}. Since upon excitation into the $^3T_{1u}$ level also emission from the $^3A_{1u}$ level is observed with an intensity comparable to that of the emission from the $^3T_{1u}$ level, the probability for the nonradiative process is of the order of magnitude as the probability for the radiative transition $^3T_{1u} \rightarrow {}^1A_{1g}$. These observations are in line with earlier results, which are gathered in Table I. From Table I it can be concluded that if two phonons are required to overcome the energy difference ΔE, the probability for the nonradiative transition $^3T_{1u} \rightarrow {}^3A_{1u}$ is larger than the radiative transition $^3T_{1u} \rightarrow {}^1A_{1g}$. If three phonons are required, these probabilities are about equal and if four phonons are required, the probability of the radiative process is larger than that of the nonradiative process.

TABLE I

THE ENERGY DIFFERENCE ΔE BETWEEN THE $^3T_{1u}$ AND THE $^3A_{1u}$ LEVELS, THE FREQUENCY OF THE ν_1 VIBRATIONAL MODE, AND THE RATIO (R) OF THESE TWO VALUES FOR SEVERAL Bi^{3+}-ACTIVATED PHOSPHORS

Compound	ΔE (cm^{-1})	ν_1 (cm^{-1})	R	Emission at 4.2 K	Reference
$ScBO_3$–Bi^{3+}	965	550	1.8	$^3A_{1u}$	*(19)*
CaO–Bi^{3+}	1180	510	2.3	$^3A_{1u}$	(25)
$Cs_2NaLaCl_6$–Bi^{3+}	800	290	2.8	$^3A_{1u}$ and $^3T_{1u}$	This work
CaS–Bi^{3+}	880	276	3.2	$^3A_{1u}$ and $^3T_{1u}$	*(26, 27)*
Cs_2NaYCl_6–Bi^{3+}	1150	290	4.0	$^3T_{1u}$	*(11)*
Cs_2NaYBr_6–Bi^{3+}	650	160	4.1	$^3T_{1u}$	This work

Comparing the luminescence properties of $Cs_2NaLaCl_6$–Bi^{3+} and Cs_2YaYCl_6–Bi^{3+} some conclusions can also be made. The Stokes shift for $Cs_2NaLaCl_6$–Bi^{3+} is larger than for Cs_2NaYBr_6–Bi^{3+}, due to the larger space available for the Bi^{3+} ion in the lanthanum lattice. Upon A band excitation, emission from the $^3T_{1u}$ level and the $^3A_{1u}$ level is observed, while for Cs_2NaYCl_6–Bi^{3+} only $^3T_{1u}$ emission is observed upon A band excitation. The energy difference ΔE between the $^3T_{1u}$ level and the $^3A_{1u}$ level is smaller in case of $Cs_2NaLaCl_6$–Bi^{3+}.

4.3. Energy Transfer in $Cs_2NaLaCl_6$–Bi^{3+}

In Fig. 8 it is seen that the quenching temperature of the luminescence of $Cs_2NaLaCl_6$–Bi^{3+} depends on the Bi^{3+} concentration. This suggests that quenching of the emission is due to energy transfer. It is possible to estimate the critical distance R_c for energy transfer. This is the distance between the Bi^{3+} ions for which the probability for energy transfer is equal to the probability for the radiative transition. The critical distance R_c is given by *(29, 30)*

$$R_c^6 = 0.63 \times 10^{-28} \cdot \frac{Q_A}{E^4} \cdot \mathrm{SO}. \qquad (1)$$

In this formula Q_A is the absorption cross section, E is the energy at which the spectral overlap is maximal and SO is the spectral overlap between the excitation band and the emission band. For energy transfer in $Cs_2NaLaCl_6$–Bi^{3+} three different processes are possible, viz., transfer between the single Bi^{3+} ions, transfer from single Bi^{3+} ions to Bi^{3+} pairs, and transfer between the Bi^{3+} pairs. From the spectral data it is possible to estimate R_c for each of these processes. The results are gathered in Table II. For these estimations it was assumed that $Q_A = 10^{-16}$ cm^2 eV. It should be realized that these are estimations of R_c only, since due to the high Bi^{3+} concentrations in

TABLE II

DATA FOR THE ENERGY TRANSFER PROCESSES IN $Cs_2NaLaCl_6$–Bi^{3+}

Transfer process	E (eV)	SO (eV^{-1})	R_c (Å)
Bi^{3+} single → Bi^{3+} single	3.70	0.07[a]	25
Bi^{3+} single → Bi^{3+} pair	3.70	1.6[b]	42
Bi^{3+} pair → pair	3.60	0.12	28

[a] The spectral overlap between the $^3T_{1u}$ emission and the excitation region.

[b] The spectral overlap between the $^3T_{1u}$ emission of the single Bi^{3+} ion and the excitation band of the Bi^{3+} pair.

the crystals, the real excitation spectra are not known. This may especially influence the data for the isolated Bi^{3+} ions. Probably the real value of R_c for the isolated Bi^{3+} ions is smaller. For energy transfer between ions on the same crystallographic sublattice it is possible to determine the critical concentration x_c. The relation between x_c and R_c is given by (*30*)

$$R_c \approx 2\left(\frac{3V}{4\pi x_c N}\right)^{1/3}. \tag{2}$$

In this equation V presents the volume of the unit cell and N the number of molecules in the unit cell. (In the case of $Cs_2NaLaCl_6$: $V = 1443$ Å^3 and $N = 4$.) The critical concentration for energy migration between the single Bi^{3+} ions is about 4 at.%. Because the Bi^{3+} concentrations in our crystals are much lower, energy migration between the isolated Bi^{3+} ions cannot occur. The most probable process is energy transfer from the isolated Bi^{3+} ion to the Bi^{3+} pairs. Quenching of the emission of the isolated Bi^{3+} ions at higher temperature is due to this process. Because quenching of the pair emission starts at lower temperature than quenching of the single Bi^{3+} ion emission, an increase of the pair emission at higher temperature cannot be observed.

Similar phenomena may be expected for Cs_2NaYBr_6–Bi^{3+}, but the low thermal quenching temperature prevents further investigations.

4.4. Comparison with Tl^+-Activated Alkali Halides

In Table III the positions of the A band (absorption/excitation) and the emission bands of some Tl^+-activated alkali halides and the system described in this chapter are gathered. From this table it is seen that for KCl–Tl^+ only one emission band (A_T) is observed. For KBr–Tl^+ and RbCl–Tl^+ two emission bands (A_T at higher energy and A_X at lower energy) are observed. The origin of these two emission bands is the existence of two minima (T and X) on the adiabatic potential energy surface (APES) of the $^3T_{1u}$ relaxed excited state (RES). Fukuda (*6*) pointed out that the existence of these two minima is determined by the expression

$$A = \frac{12\xi(1-\beta)}{b^2}. \tag{3}$$

In this equation, ξ presents the spin–orbit interaction, β the difference in curvature between the ground state and the excited state APES, and b^2 the electron–lattice interaction. It is difficult to determine these parameters. A rough estimate of these values is (*6*) $\xi = 0.1$–0.7 eV, $\beta = 0.1$–0.6 eV, and $b^2 = 0.8$–3 eV. The ratio A determines the relative depth of the T and X minima. Fukuda distinguishes three cases: (1) The X

TABLE III

SPECTRAL DATA OF SOME Tl^+-ACTIVATED ALKALI HALIDES AND OF THE SYSTEMS DESCRIBED IN THIS CHAPTER

Compound	Absorption/ excitation (eV)	Emission (eV)	Reference
KCl–Tl^+	5.03	4.17 (A_T)	(*6, 7*)
KBr–Tl^+	4.79	4.02 (A_T) 3.50 (A_x)	(*6, 7*)
RbCl–Tl^+	5.06	3.95 (A_T) 3.53 (A_x)	(*6, 7*)
Cs_2NaYCl_6–Bi^{3+}	3.80	3.72 ($^3T_{1u}$)	This work
Cs_2NaYBr_6–Bi^{3+}	3.36	3.16 ($^3T_{1u}$)	This work
$Cs_2NaLaCl_6$–Bi^{3+}	~3.9	3.63 ($^3T_{1u}$)	This work

minimum is sufficiently deeper than the T minimum (only A_X emission observed). (2) The depth of the X minimum is about equal to the depth of the T minimum) A_T and A_X emission observed). (3) The X minimum does not exist (only A_T emission observed). For small values of A (~ 1) case (1) is observed, for larger values of A case (2), and finally for large values of A case (3). This is demonstrated by the data in Table II on the Tl^+-activated alkali halides. The system $KCl-Tl^+$ is an illustration of case (3). The parameters β and b^2 increase on going from KCl to KBr and also on going from KCl to RbCl, while ξ does not change much (*6, 7*) and we arrive at case (2). The value of ξ is known to increase on going from Tl^+ to Bi^{3+} (*6, 21*) and the value of b must decrease in view of the vibrational structure in the spectra of the Bi^{3+}-activated compounds. This implies that A must be much larger for the Bi^{3+}-activated compounds than for the Tl^+-activated alkali halides. This accounts for the observation of only A_T emission in the former case and makes it highly improbable that A_X emission from the Bi^{3+} ion can be observed at all.

Acknowledgments

The authors are indebted to Mr. G. J. Dirksen for the crystal growth of $Cs_2NaYBr_6-Bi^{3+}$ and $Cs_2NaLaCl_6-Bi^{3+}$ and for the analysis of the crystals. We are also indebted to Dr. C. W. M. Timmermans for providing crystals of $Cs_3Bi_2Br_9$ and $Cs_3Bi_2Cl_9$.

References

1. G. Blasse and A. Bril, *J. Chem. Phys.* **48,** 217 (1968).
2. G. Boulon, *J. Phys. (Orsay, Fr.)* **32,** 333 (1971).
3. G. Boulon, C. Pedrini, M. Guidoni, and Ch. Pannel, *J. Phys. (Orsay, Fr.)* **36,** 267 (1975).
4. A. C. van der Steen, J. J. A. van Hesteren, and A. P. Slok, *J. Electrochem. Soc.* **128,** 1327 (1981).
5. C. W. M. Timmermans and G. Blasse, *J. Solid State Chem.* **52,** 222 (1984).
6. A. Fukuda, *Phys. Rev. B* **1,** 4161 (1970).
7. A. Ranfagni, D. Mugnai, M. Bacci, G. Villiani, and M. P. Fontana, *Adv. Phys.* **32,** 823 (1983).
8. L. R. Morss and J. Fuger, *Inorg. Chem.* **8,** 1433 (1964).
9. D. Babel, R. Haegle, G. Pausewang, and F. Wall, *Mater. Res. Bull.* **8,** 1371 (1973).
10. L. R. Morss, M. Siegal, L. Stenger, and N. Edelstein, *Inorg. Chem.* **9,** 1771 (1970).
11. A. C. van der Steen, *Phys. Status Solidi B* **100,** 603 (1980).
12. G. Meyer and H. C. Gaebell, *Z. Naturforsch.* **336,** 1476 (1978).
13. R. W. Schwartz, S. W. Watkins, C. J. O'Connor, and R. L. Carlin, *J. Chem. Soc. Faraday Trans. 2* **72,** 565 (1976).
14. A. C. van der Steen and G. J. Dirksen, *Chem. Phys. Lett.* **59,** 110 (1978).
15. C. W. M. Timmermans and G. Blasse, *Phys. Status Solidi B* **106,** 647 (1981).
16. C. W. M. Timmermans, S. O. Cholakh, and G. Blasse, *J. Solid State Chem.* **46,** 222 (1983).
17. A. Bril and A. W. de Jager-Venis, *J. Electrochem. Soc.* **123,** 396 (1976).
18. A. Wolfert and G. Blasse, *Mater. Res. Bull.* **19,** 67 (1984).
19. A. Wolfert, W. E. J. L. Oomen, and G. Blasse, *J. Solid State Chem.*, in press.
20. Hao Zhiran and G. Blasse, *Mater. Chem. Phys.* **12,** 257 (1985); *J. Lumin.* **31/32,** 817 (1984).
21. C. K. Jørgensen, "Absorption Spectra and Chemical Bonding in Complexes," p. 186, Pergamon, New York (1962).
22. C. W. M. Timmermans and G. Blasse, *Phys. Status. Solidi B* **118,** 353 (1983).
23. A. Wolfert and G. Blasse, *J. Lumin.* **33,** 213 (1985).
24. A. Wolfert and G. Blasse, *J. Solid State Chem.* **55,** 344 (1984).
25. A. C. van der Steen and L. T. F. Dijcks, *Phys. Status Solidi B* **104,** 283 (1981).
26. N. Yamashita and S. Asano, *J. Phys. Soc. Japan* **40,** 144 (1976).
27. T. Ohata, T. Hayaski, and S. Koshino, *J. Phys. Soc. Japan* **45,** 581 (1978).
28. Le Si Dang, R. Romestain, D. Simkin, and A. Fukuda, *Phys. Rev. B* **18,** 2989 (1978).
29. D. L. Dexter, *J. Chem. Phys.* **21,** 836 (1953).
30. G. Blasse, *Philips Res. Rep.* **24,** 131 (1969).